Environmental Science and Pollution Research
https://doi.org/10.1007/s11356-022-23508-5

RESEARCH ARTICLE

Evaluation of the protective effects of berberine and berberine nanoparticle on insulin secretion and oxidative stress induced by carbon nanotubes in isolated mice islets of langerhans: an in vitro study

Fereshteh Golfakhrabadi[1,2] · Mohammad Reza Niknejad[3,4] · Heibatullah Kalantari[3,4] · Mohammad Amin Dehghani[3,4] · Nader Shakiba Maram[5,6] · Akram Ahangarpour[7]

Received: 11 October 2021 / Accepted: 4 October 2022

Abstract

The increasing use of single-walled carbon nanotubes (SWCNT) in various fields highlights the need to investigate the test toxicity of these nanoparticles in humans. Previous documents showed that SWCNT induced oxidative stress. Oxidative stress and reactive oxygen species (ROS) cause cell dysfunction and reduced insulin secretion. Therefore, this study aimed to investigate the effects of SWCNT on oxidative stress and insulin secretion of islets also evaluate the protective effects of berberine (BBR) and berberine nanoparticles (NP-BBR) as antioxidants on pancreatic β-islets. Double emulsion with solvent evaporation was the technique used to prepare nanoparticles in this study. Islets were isolated and pretreated with various concentrations of BBR and NP-BBR and then treated with single dose of SWCNT (160 µg). The results of this study showed that SWCNT decreased cell viability based on MTT assay, reduced insulin secretion of islets, increased malondialdehyde (MDA) amounts, reactive oxygen species (ROS) levels, reduced glutathione (GSH) levels, catalase (CAT), superoxide dismutase (SOD), and glutathione peroxidase (GPx) activities, whereas pretreatment of islets with low doses of BBR (5 and 15 µM) and NP-BBR (5 µM) significantly reversed all changes induced by SWCNT. These findings suggested that SWCNT might trigger other pathways involved in insulin secretion by activating the oxidative stress pathway in the pancreatic islets, reducing insulin secretion, consequently diabetes. BBR and NP-BBR as antioxidants were able to protect pancreatic β-islets and prevent the progression of diabetes.

Keywords Single-walled carbon nanotubes · Berberine nanoparticles · Oxidative stress · Islet insulin secretion · Diabetes

Responsible Editor: Mohamed M. Abdel-Daim

✉ Akram Ahangarpour
akramahangarpour@gmail.com

[1] Department of Pharmacognosy, Faculty of Pharmacy, Nanotechnology Research Center, Ahvaz Jundishapur University of Medical Sciences, Ahvaz Jundishapur University of Medical Sciences, Ahvaz, Iran

[2] Medicinal Plant Research Center, Medical Basic Sciences Research Institute, Ahvaz Jundishapur University of Medical Sciences, Ahvaz, Iran

[3] Department of Toxicology, School of Pharmacy, Ahvaz Jundishapur University of Medical Sciences, Ahvaz, Iran

[4] Medical Basic Sciences Research Institute, Toxicology Research Center, Ahvaz Jundishapur University of Medical Sciences, Ahvaz, Iran

[5] Nanotechnology Research Center, Ahvaz Jundishapur University of Medical Sciences, Ahvaz, Iran

[6] Department of Pharmaceutics, School of Pharmacy, Ahvaz Jundishapur University of Medical Sciences, Ahvaz, Iran

[7] Department of Physiology, Faculty of Medicine, Diabetes Research Center, Health Research Institute, Ahvaz Jundishapur University of Medical Sciences, Ahvaz, Iran

Published online: 24 October 2022

Introduction

Carbon nanotubes (CNTs) are among the materials that have attracted much research attention because of their potential new approaches to diagnosing, treating diseases, and inspiring new ideas in medicine Whitesides 2003. CNTs are hollow graphene cylinders between a few microns and a few millimeters long and can be divided into two groups: single-walled CNTs (SWCNT) with a diameter of 0.7 to 3 nm and multi-walled CNTs (MWCNT) with a diameter of 10 to 25 nm Baughman et al. 2002. Human contact can occur unintentionally in industry or when CNTs are used as a therapeutic and diagnostic tool in the treatment of human diseases. CNTs, due to their smaller size than cellular organelles, can penetrate into cells and organelles in the process of production or use as a therapeutic or diagnostic tool and cause toxicity in them, thus determining the potential toxicity of CNTs essential in cells. Toxicology studies have been performed in vivo and in vitro on CNTs. Studies exhibited that human contact to CNTs caused genetic damage, apoptosis, cell dysfunction, increased membrane disruption, reduced cell adherence, and induced oxidative stress Shvedova et al. 2003; Kagan et al. 2006; Bottini et al. 2006. Previous studies in vitro and in vivo have shown that CNTs induce cellular toxicity also acute and chronic inflammatory responses in organs. The toxicity of CNTs is associated with their physicochemical properties including shape, purity, length, size, surface functionalization, and agglomeration Allegri et al. 2016; Jos et al. 2009; Ong et al. 2016; Thompson et al. 2015. After entering cells, SWCNT cause oxidative stress through ROS generation, which is one of the effective factors for increasing apoptosis and cell death. SWCNT also reduce the antioxidant defense system of cells and mitochondria Cheng et al. 2011. Augmented oxidative stress may be a trigger for other molecular pathways that lead to pancreatic β-cell dysfunction, insulin resistance, dyslipidemia, reduced glucose tolerance, and eventually type 2 diabetes. Chronic oxidative stress is destructive to β cells because oxidative stress consumes a lot of energy and lowers antioxidant levels. Thus, the expression of key genes in β-cells is reduced and the genes involved in apoptosis are activated, causing cell death Tangvarasittichai 2015. B-cells have the protective enzymes catalase (CAT) and superoxide dismutase (SOD) on a smaller scale than other tissues, and are therefore more sensitive to oxygen-free radicals and oxidative stress Vessby et al. 2002; Wolf et al. 2010. According to previous studies and the identification of the destructive effects of oxidative stress on β-cells and the progression of diabetes, it is concluded that the use of antioxidants to reduce the adverse effects of oxidative stress can be used as an effective method in the treatment and prevention of diabetes. Berberine (BBR) is an isoquinoline alkaloid derived from the Chinese plant *Coptis chinensis*, which is used in traditional Chinese medicine to treat diarrhea Ceriello & Testa 2009. The effects of BBR on lowering blood sugar and blood lipids, regulating the immune system, reducing inflammation and antitumor, antioxidant, and scavenging ROS have been studied Johansen et al. 2005. Studies have suggested that BBR protected the heart by maintaining Ca^{+2} homeostasis, inhibiting calpain, the activation of phosphoinositide-3 kinase, protein kinase B enzymes, leading to inhibition of the glycogen synthetase kinase-3β (GSK 3β), and opening the mitochondrial ATP-sensitive K channels Abushouk et al. 2017. The low bioavailability of BBR is a problem in its clinical prescription. Consequently, the development of a system is required to enhance the physical and chemical characteristics of BBR including increasing its half-life, bioavailability, and solubility for better clinical use. Nanoparticles have proven to be a good way to overcome these problems. Various studies have shown the effectiveness and increased bioavailability of nanoparticle-BBR (NP-BBR) in platforms based on polymer, carbon, lipid, and metal Chen et al. 2016; Mirhadi et al. 2018; Poupot et al. 2018.

In this study, the double emulsion-solvent evaporation used as a proper technique for preparing NP-BBR and Eudragit RS-100 as a biocompatible polymer with widespread applications in oral dosage forms. This study aimed to investigate the possible protective effects of BBR and NP-BBR against SWCNT-induced oxidative stress in mice pancreatic islets.

Materials and methods

Chemicals

SWCNT (length 50–300 nm and diameter 1–2 nm) were obtained from USA Research Nanomaterials, Inc. (Houston, TX 77,084, USA). BBR, MTT, ethylene glycol tetraacetic acid (EGTA), 4-(2-hydroxyethyl)-1-piperazineethanesulfonic acid) (HEPES), Coomassie Brilliant Blue powder, 2,7-dichlorofluorescein diacetate (DCFH-DA), thiobarbituric acid (TBA), trichloroacetic acid (TCA), RPMI-1640 media (R8758), and 1,1,3,3-tetramethoxypropane were obtained from Sigma-Aldrich, Co. (St Louis, MO, USA). Dimethyl sulfoxide (DMSO) and 5, 50—dithiobis (2—nitrobenzoic acid) (DTNB) were obtained from Merck, Co. (Darmstadt, Germany). Other required high-purity chemicals were procured from the market.

Animals

This experimental study was performed on adult male NMRI mice prepared from Ahvaz Jundishapur University

of Medical Sciences, Ahvaz, Iran. Mice in groups of 5 were protected in cages with water, food, heat of 22 ± 2 °C, and 12-h cycle of light and dark. Conditions for keeping and working with animals have been done according to the instructions of the Animal Ethics Committee of Ahvaz Jundishapur University of Medical Sciences (confirmation number: IR.AJUMS.REC. 1397–035).

Characterization of nanoparticles

Preparation of NP-BBR

Double emulsion with solvent evaporation was the technique used to prepare nanoparticles in this study. First, to prepare the aqueous phase, BBR (200 mg) was added to distilled water (30 ml) and dissolved well, then to prepare the organic phase, Eudragit RS-100 (400 mg) was added to dichloromethane (40 ml) and dissolved well. During homogenization, the aqueous phase was poured on the organic phase. Again in the container containing ice, during homogenization, prepared emulsion (W1/O) was added to polyvinyl alcohol (PVA, 100 ml, 0.2%) to obtain emulsion (W1/O/W2), which was agitated for 3 h. The final emulsion was centrifuged for 30 min and obtained supernatant was then collected.

Production yield

The nanoparticles were lyophilized after obtaining the abovementioned steps and the yield of the product was calculated according to the following equation:

$$\begin{aligned} Production\ yield = (Weight\ of\ freeze\ dried\ nanoparticles\ (mg)) \\ /(Weight\ of\ drug\ (mg) + Polymer\ (mg)) \times 100 \end{aligned} \quad (1)$$

Loading efficiency

The loading efficiency of drug was determined by extracting the drug using phosphate-buffered saline (PBS). NP-BBR suspension was centrifuged at 6000 × g for 30 min at 25 °C, then 10 ml of the supernatant containing unloaded BBR was placed in the dialysis bag. The bag was then placed in a becher containing 20 ml of PBS. The becher was stirred on a magnetic stirrer for 30 min (50 × g) at room temperature to let the solutions become equilibrated with each other. Finally, the absorption of unloaded BBR was measured by spectrophotometry, Shimadzu (Kyoto, Japan), at 420 nm. Entrapment efficiency (EE %) was calculated using the following formulation:

$$\begin{aligned} EE\% = &(amount\ of\ drug\ in\ the\ formulation\ (mg) - amount\ of\ unloaded\ drug\ in\ supernatant\ (mg)) \\ &/(amount\ of\ drug\ in\ the\ formulation\ (mg)) \times 100 \end{aligned} \quad (2)$$

Nanoparticle size analysis

After diluting NP-BBR in double-distilled water, the size of NP-BBR was examined by a particle size analyzer (Scatter scope 1 Qudix, South Korea). Each test was performed three times and an average of three was reported.

Scanning electron microscopy

In this study, SEM was used to determine the surface morphology of NP-BBR. The suspension containing 2 mg of NP-BBR was spread on an aluminum sheet. After drying, it was surrounded with gold/palladium (50 nm) and the surface morphology of NP-BBRs was observed under an electron microscope (Leo 1455 VP, Germany).

Fourier transform infrared spectroscopy

FT-IR was used to identify functional groups of nanoparticles by varying their wave number. FT-IR of NP-BBR, BBR, and Eudragit RS was done by an IR spectroscope equipment using KBr disks over a range of 500–4000 cm^{-1} to determine the functional groups and the reaction between the drug and the polymer.

Zeta potential determination

Zeta potential measures the potential difference between a liquid in which a particle is dispersed and a layer of liquid containing oppositely charged ions related with the surface of nanoparticles and the value of the zeta potential provides information about the stability of the particles. For this purpose, nanoparticles were suspended in distilled water with pH = 7 at room temperature. The surface charge of samples was performed three times and the average of them was reported as zeta potential by a Zetasizer (Malvern, ZEN3600, UK) device.

Thermogravimetric analysis studies of nanoparticles

TGA is used to measure the level of coating on the surface of nanoparticles. In this study, TGA of NP-BBR, BBR, and Eudragit RS-100 was done using Chromatopac R6A (Shimadzu, Japan). Five milligrams of each of these compounds was transferred to an aluminum surface and scanned from 50 to 1150 °C at a heating rate of 10 °C/min, and an empty aluminum pan was used as the negative control group.

Drug release assay

The USP II Paddle was used to determine the BBR release profile of the NP-BBR. For this purpose, 20 mg of NP-BBR was added to 200 ml of PBS and kept in dialysis bag with 10,000 Daltons. The tests were performed in the first half hour, one, two, three, four, five, six, eight, twelve, and 24 h. Five milliliters was taken from each sample and the existence of BBR was measured using a UV spectrophotometer at a wavelength of 240 nm Anitha et al. 2011.

Isolation islets

The mice pancreatic islets were first separated and then isolated by collagenase digestion method. The bile duct at the distal end was closed to inject 5 ml of Hank's Balanced Salt Solution (HBSS) into it. The compounds of HBSS include NaH2PO4, 1.2 mmol/l, D-glucose 5 mmol/l, CaCl2 2.5 mmol/l, NaCl 115 mmol/l, MgCl2 1.1 mmol/l, HEPES 25 mmol/l, NaHCO3 10 mmol/l, and KCl 5 mmol/l that BSA 1% and collagenase P 1.4 mg/ml with PH 7.4 were added to the duct. The pancreas were removed and then placed into a tube and incubated for 20 min in a water bath (37 °C). In the next step, 15 ml of HBSS was added to the tubes to weaken the collagen and prevent more ingestion. The tubes were centrifuged for 5 min at 1500 rpm to wash away the collagenase from islet. The isolated islets were transferred to a Petri dish. The islets were disconnected by handpicking under a stereomicroscope. The islets were cultured in RPMI-1640 media along with 5 mM D-glucose, fetal calf serum (10%), penicillin and streptomycin (each 100 U/ml), 95% O2, and five % CO2 (Carter et al. 2009; Quesada et al. 2006).

Insulin secretion assessment

Insulin secretion was monitored using static glucose incubation. The islets were pre-incubated overnight in RPMI medium. The mice-isolated islets were divided into 36 groups (ten islets in each group), 12 groups for concentration of 2.8 mM glucose, 12 groups for concentration of 5.6 mM glucose, and 12 groups for concentration of 16.7 mM glucose.

Group 1: Islets were cultured in RPMI-1640 medium for 48 h (as the control group).
Group 2: Islets were cultured for 24 h in RPMI-1640 medium then treated with 50 µM of H2O2 for 2 h.
Group 3: Islets were cultured for 24 h in RPMI-1640 medium then treated with 160 µg of SWCNT for 24 h.
Group 4: Islets were pretreated with 10 µg of glibenclamide (GLIB) in RPMI-1640 medium for 24 h and then exposed with 160 µg of SWCNT for 24 h.
Group 5: Islets were pretreated with 5 µM of BBR in RPMI-1640 medium for 24 h and then treated with 160 µg of SWCNT for 24 h.
Group 6: Islets were pretreated with 15 µM of BBR in RPMI-1640 medium for 24 h and then treated with 160 µg of SWCNT for 24 h.
Group 7: Islets were pretreated with 45 µM of BBR in RPMI-1640 medium for 24 h and then treated with 160 µg of SWCNT for 24 h.
Group 8: Islets were pretreated with 5 µg of NP-BBR in RPMI-1640 medium for 24 h then treated with 160 µg of SWCNT for 24 h.
Group 9: Islets were pretreated with 15 µg of NP-BBR in RPMI-1640 medium for 24 h then treated with 160 µg of SWCNT for 24 h.
Group 10: Islets were pretreated with 45 µg of NP-BBR in RPMI-1640 medium for 24 h then treated with 160 µg of SWCNT for 24 h.
Group 11: Islets were treated with 45 µg of BBR in RPMI-1640 medium for 48 h.
Group 12: Islets were treated with 45 µg of NP-BBR in RPMI-1640 medium for 48 h.

After the end of treatment, the islets were washed with HBSS and 1 ml RPMI-1640 medium including concentrations of 2.8, 5.6, and/or 16.7 mM glucose was poured on islets and was incubated at 37 °C for 1 h. After the treatment period, the samples were centrifuged and the supernatant was used to measure insulin levels. Insulin amounts of samples were evaluated using a Rat Insulin ELISA kit (Monobind, USA) and the data were presented as µU/islet/h (Ahangarpour et al. 2018).

Islet viability test

The islet viability was measured by MTT test. First, the islets were treated with different doses of SWCNT (40, 80, 160, and 320 µg), and then based on the MTT method, the dose of 160 µg was selected as the toxic dose. In the next step, the islets were pre-treated with different doses of BBR (5, 15, and 45 µM) and NP-BBR (5, 15, and 45 µM) and treated with a single dose of SWCNT (160 µg) then the MTT assay was performed. Concisely, the islet pre-treatment groups were first eluted by Krebs-HEPES buffer and the MTT (20 ml) was poured on the samples and incubated at 37 °C for 1 h, then 100 ml of dimethyl sulfoxide again was added to samples and their absorbance were read at 570 nm by an ELISA reader. The viability of control group was considered as 100% and the rest of the groups were calculated relative to the percentage of the control, H2O2 50 µM group, as the positive control group was considered Hosseini et al. 2013.

Preparation of islets

The islets were separated into 36 groups (ten islets in each group) and exposed with different doses of BBR, NP-BBR, and SWCNT (160 µg). After the end of the treatment, the islets were again divided into three groups: 12 groups for concentration of 2.8 mM glucose, 12 groups for concentration of 5.6 mM glucose, and 12 groups for concentration of 16.7 mM glucose. Finally, the islets were exposed to a concentrations of 2.8, 5.6, and/or 16.7 mM of glucose for 1 h, then the islets were eluted with PBS (3 times), lysed, and then centrifuged for 15 min at 4 °C Xiong et al. 2006).

Biochemical tests and protein measurement

First, the islet protein content was measured by the Bradford method. One milliliter of Bradford reagent was poured on homogenized islets (20 ml) and the absorbance of samples was immediately detected at 595 nm. The absorbance of BSA was read as the standard protein concentration Bradford 1976. After determining the protein, the levels of MDA, GSH, GPx, CAT, and SOD were measured by specific commercial kits from Beyotime Institute of Biotechnology (Jiangsu, China).

ROS level measurement

The levels of ROS of islets were measured by DCFH-DA. In summary, 36 treatment and pretreatment groups were eluted with PBS and then 40 mM of DCFH-DA was added to them and incubated for 30 min at 37 °C. After incubation, the islets were again eluted with PBS and lysed with NaOH. Finally, fluorescent intensity produced by oxidation of DCFH-DA was detected by an ELISA fluorimeter in 485 and 530 nm (excitation and emission respectively) Ahangarpour et al. 2017.

Statistical analysis

In this study, the data were evaluated by GraphPad Prism software program (version 5.04). Data were calculated as mean ± standard deviation (SD) with one-way analysis of variance (ANOVA) followed by Tukey's post hoc test. Significant differences were considered at $P < 0.05$.

Results

Production yield and loading efficiency

In this study, NP-BBR was synthesized by double emulsions-solvent evaporation method. As shown in Table 1, the production yield of NP-BBR was 88.43 ± 7.15, which was an acceptable formulation production yield. As shown in Table 1, the loading efficiency of NP-BBR was determined 84.95 ± 7.75, which was an acceptable formulation loading efficiency. This suggested that increasing the ratio of polymer to the drug, more particles of the drug were stuck inside nanoparticles.

Particle size

As observed, the average particle size of the formulation is shown in Fig. 1. The mean particle size was 168 ± 14.6 nm. A similar study to our study showed that size of nanoparticles in the formulation of Eudragit RS-100 to drug was 1:1 and 3:1 Barzegar-Jalali et al. 2012; Nath et al. 2011. As revealed in Table 1, the mean polydispersity index (PDI) of the formulation was 0.28 ± 0.024, which was adequate for polymer-based nanoparticles Danaei et al. 2018.

SEM

As the SEM images shown in Fig. 2, the NP-BBR had a sphere-shaped and moderately uniform surface.

FT-IR

According to the FT-IR spectra (Fig. 3A, B, and C), the existence of a peak at 1744 cm^{-1} showed the existence of a steric carbonyl group due to the presence of polymer in the nanoparticles. Also, existence of peaks at 1475–1635 cm^{-1} approved the presence of BBR in the nanoparticles.

Zeta potential

As observed in Fig. 4, the zeta potential of NP-BBR, BBR, and Eudragit RS-100 were detected as + 30.6, − 40.7, and + 40.4, respectively. Because the surface charge of the Eudragit RS-100 was positive, the encapsulation of the BBR in the Eudragit RS-100 was recognized (Zhang et al. 2014). The zeta potential of the formulation indicated that the nanoparticles had good stability.

TGA

As observed in Fig. 5A, B, and C, the agents were heated from 50 to 1150 °C at the rate of 10 °C/min. As results showed, the

Table 1 The production efficiency, loading yield mean particle size and PDI

Mean production yield ± SD (%)	Mean loading efficiency ± SD (%)	Mean particle size mean ± SD (nm)	Mean PDI ± SD
88.43 ± 7.15	84.95 ± 7.75	168 ± 14.6	0.28 ± 0.024

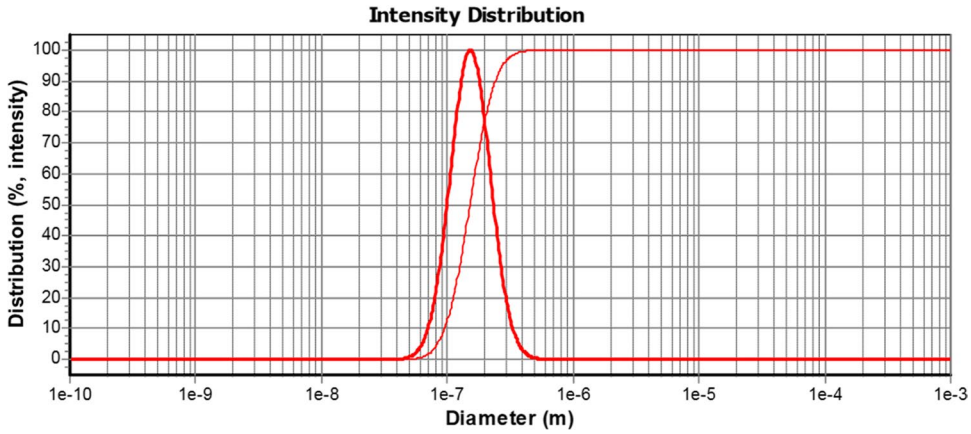

Fig. 1 The nanoparticle size diagram

peak of 147 °C was associated with the melting point of the BBR, but the existence of a peak shorter in comparison with BBR indicated the existence of the polymer in the NP-BBR that this showed the thermal stability of the prepared nanoparticle.

Dissolution test in PBS

As observed in Fig. 6, approximately 20% of BBR at 30 min was released that this burst release usually happens in all the microspheres ready by the solvent evaporation method Beck et al. 1979; Bodmeier & McGinity 1988; Huang & Ghebre-Sellassie 1989; Jeyanthi & Rao 1989; Kojima et al. 1984; Nishioka et al. 1990; Ogawa et al. 1988; Seki et al. 1990; Singh & Robinson 1988; Suzuki & Price 1985; Uchida et al. 1992; Wada et al. 1990. Burst release can cause faster and better drug penetration while sustained release of the drug over a long period of time will deliver the drug to the site of absorption Bhaskar et al. 2009. One study reported that the incomplete ibuprofen is released from Eudragit RS-100 microspheres ready by the solvent evaporation technique Armand et al. 1987; Babay et al. 1988; Kazuhiko et al. 1986; Mady 2017; Uchida et al. 1992. This could occur for several reasons: one because of drug-polymer interactions Armand et al. 1987; Mady 2017, other reason the delay property of the polymer or the hydrogen bonding interactions Babay et al. 1988; Spenlehauer et al. 1986.

Response—dose of SWCNT

To acquire the most effective dose of SWCNT, first the islets were pretreated with different doses of SWCNT (40, 80, 160, and 320 µg) for 24 h then the viability of islets was performed by the MTT test. The islet viability of the control group was considered 100% then treatment, pre-treatment, and the positive control group (H2O2 50 µM) were compared to it. Cell viability of 40 µg of SWCNT was 94.6%, which showed a decreasing trend compared to the control group, but was not statistically significant. Cell viability of 80 µg of SWCNT was 84.8%, which showed a significant decrease compared to the control group ($P < 0.01$). Cell viability of 160 µg of SWCNT was 48.8%, and cell viability of 320 µg of SWCNT was 40.3%, which showed a significant decrease in both

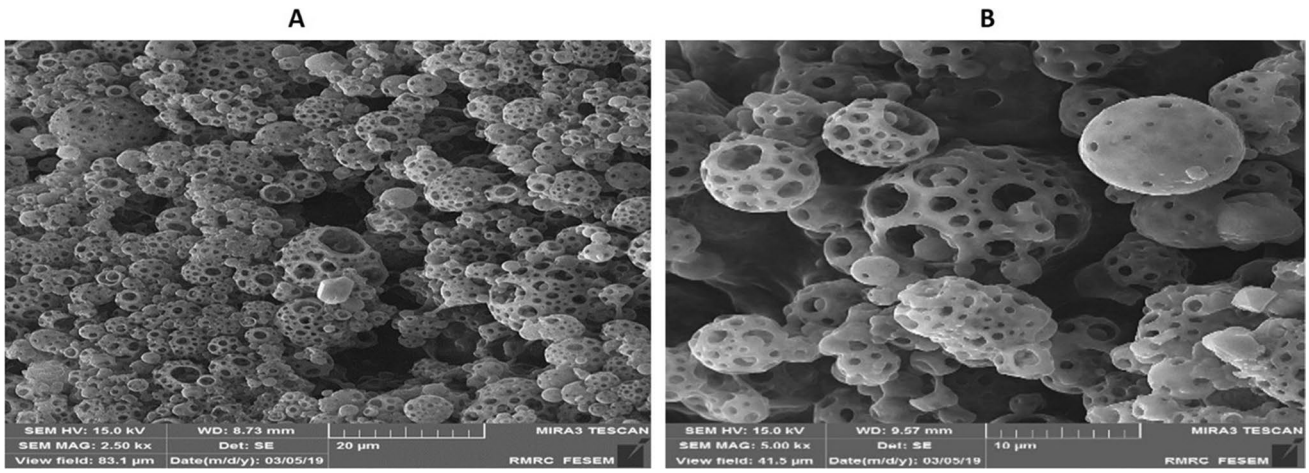

Fig. 2 SEM images of NP-BBR: **A** 20 µm and **B** 10 µm

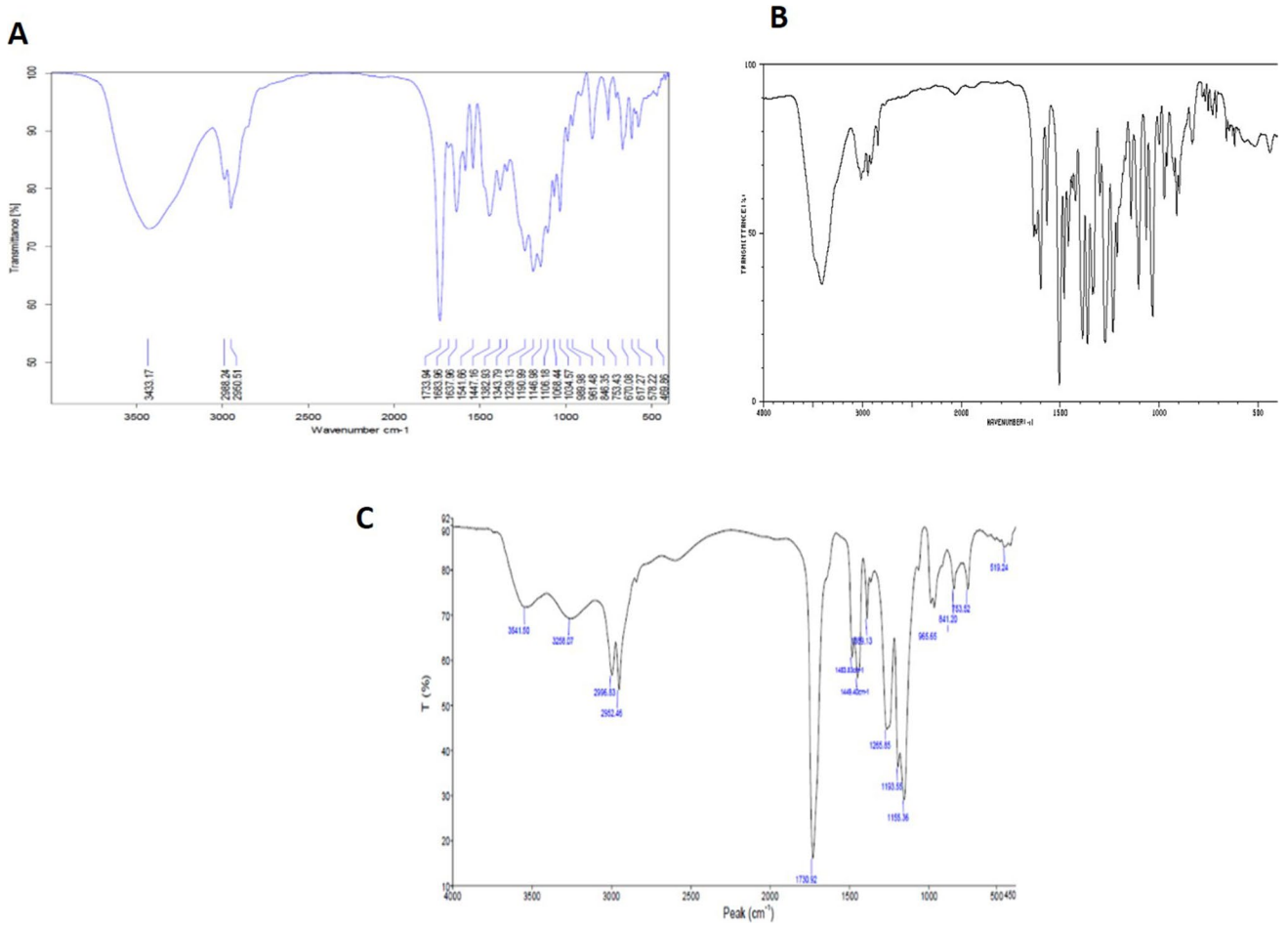

Fig. 3 **A** FT-IR spectrum of NP-BBR. **B** FT-IR spectrum of BBR. **C** FT-IR spectrum of Eudragit RS-100

groups compared to the control group ($P < 0.001$). Among all groups used, islet viability was reduced by about 50% with SWCNT (160 µg). Consequently, 160 µg of SWCNT was considered the most effective dose (Fig. 7).

Effects of BBR and NP-BBR on cell viability

After obtaining the most effective dose of SWCNT in 24 h, the islets were pretreated with different doses of BBR (5, 15, and 45 µM) and NP-BBR (5, 15, and 45 µM) then treated with a single dose of SWCNT (160 µg). As shown in Fig. 8, among all the groups used, the lowest islet viability was related to SWCNT (160 µg), which was about 50% lower than the control group almost similar to the positive control group (H2O2 50 µM) ($P < 0.001$). While pretreatment with 5 µM of BBR increased cell viability (66.5%), 45 µM of BBR increased cell viability (60.7%), and 15 µM of NP-BBR increased cell viability (60.4%), which showed a significant increase compared

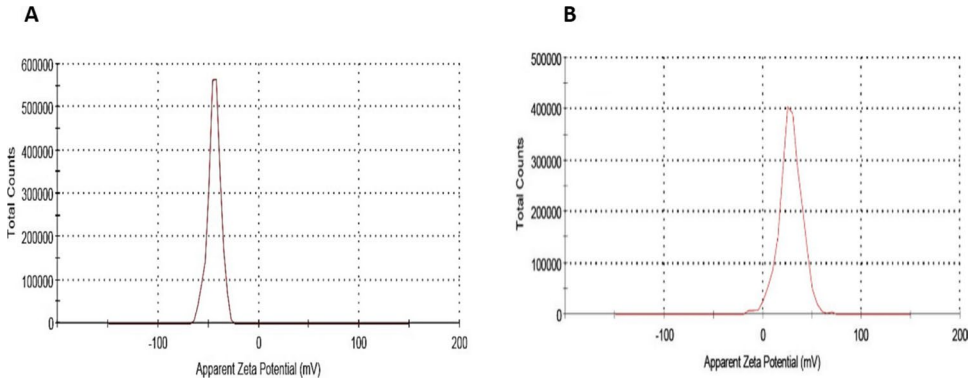

Fig. 4 Zeta potential of BBR and NP-BBR

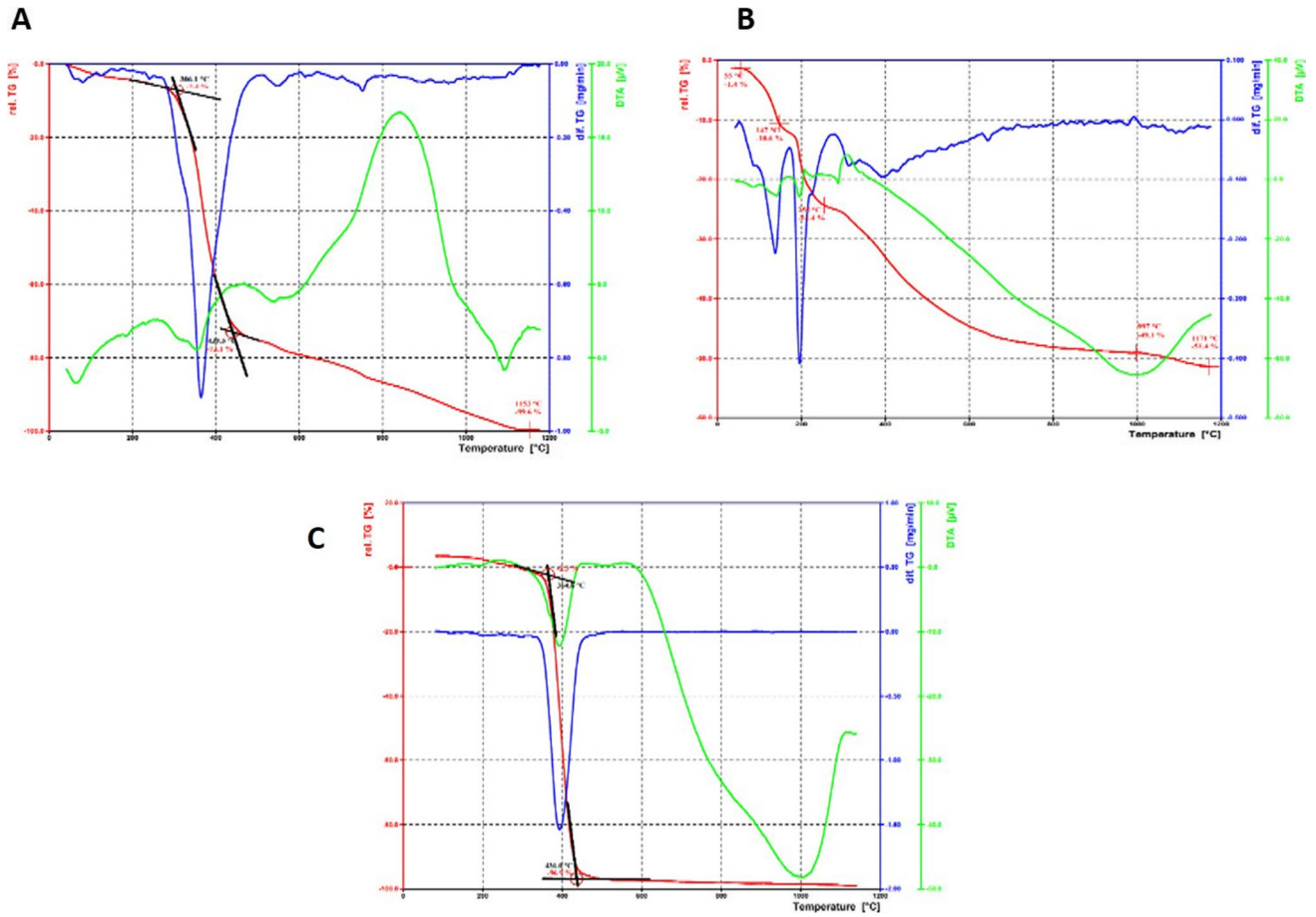

Fig. 5 **A** TGA of NP-BBR. **B** TGA of BBR. **C** TGA of Eudragit RS-100

to the SWCNT (160 µg) group alone ($P < 0.01$, $P < 0.05$, and $P < 0.05$, respectively). Fifteen micromolars of BBR and 5 µM of NP-BBR increased cell viability (83.6%) and (90.8%), respectively, which was a significant increase compared to the SWCNT (160 µg) group alone ($P < 0.001$) (Fig. 8).

Effects of BBR and NP-BBR on insulin secretion

As shown in Fig. 9a, 2.8 mM glucose pointedly augmented insulin secretion in the pretreatment groups of BBR (15 µM) and NP-BBR (5 µM) ($P < 0.01$ and $P < 0.001$). As shown in

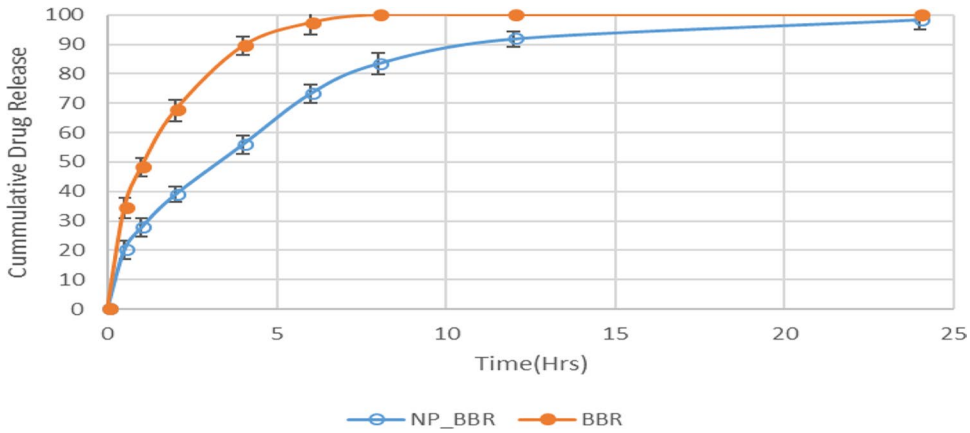

Fig. 6 Release profile of NP-BBR in phosphate buffer (pH = 7.4)

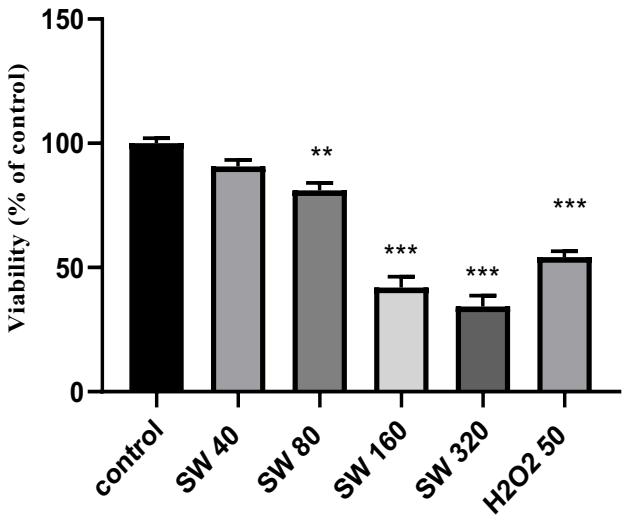

Fig. 7 Effects of SWCNT treatment on the viability of isolated mice islets. Islets were exposed to SWCNT (40, 80, 160, and 320 μg) for 24 h or H2O2 50 μM for 2 h, and then cell viability was measured. Results were represented as mean ± SD

Fig. 9b, 5.6 mM glucose significantly enlarged insulin secretion in the pretreatment groups of BBR (5, 15, and 45 μM) and NP-BBR (5 and 15 μM) ($P < 0.05$, $P < 0.01$, and $P < 0.001$). As shown in Fig. 9c, 16.7 mM glucose significantly enhanced insulin secretion in the pretreatment groups of BBR (5, 15, and 45 μM) and NP-BBR (5 and 15 μM) ($P < 0.05$ and $P < 0.001$).

Effects of BBR and NP-BBR on ROS levels

As observed in Fig. 10, islet contact to SWCNT pointedly augmented the ROS generation in comparison with the control group ($P < 0.001$). Nevertheless, the pretreatment with BBR (5, 15, and 45 μM) ($P < 0.01$ and $P < 0.05$, respectively) and NP-BBR (5 and 15 μM) ($P < 0.001$ and $P < 0.05$, respectively) significantly reduced ROS levels in comparison with the SWCNT group alone.

Effect of BBR and NP-BBR on GSH levels

As shown in Tables 2, 3, and 4; GSH levels exhibited an important reduction in SWCNT (160 μg) group alone in comparison with the control group ($P < 0.001$). While in the concentrations of glucose 2.8 and 5.6 μM, BBR (5, 15, and 45 μM) and NP-BBR (5 and 15 μM) and GLIB 10 μM significantly improved GSH levels in comparison with the SWCNT (160 μg) group alone ($P < 0.05$, $P < 0.01$, and $P < 0.001$). But in the concentration of glucose 16.7 μM, BBR (15 μM) and NP-BBR (5 μM) could improve GSH levels in comparison with the SWCNT (160 μg) group alone ($P < 0.01$ and $P < 0.001$).

Effect of BBR and NP-BBR on SOD activity

SOD activity of islet pointedly reduced in the SWCNT group alone in comparison with the control group ($P < 0.001$). In the concentration of 2.8 mM glucose, SOD activity significantly increased in BBR 5, 15, and 45 μM ($P < 0.05$, $P < 0.01$, and $P < 0.001$) as well as NP-BBR 5 μM ($P < 0.001$) (Table 2). In the concentration of 5.6 mM glucose, SOD activity significantly increased in BBR 5, 15, and 45 μM ($P < 0.05$, $P < 0.01$, and $P < 0.001$) as well as NP-BBR 5 and 15 μM ($P < 0.05$ and $P < 0.001$) (Table 3). In 16.7 mM glucose, a protective

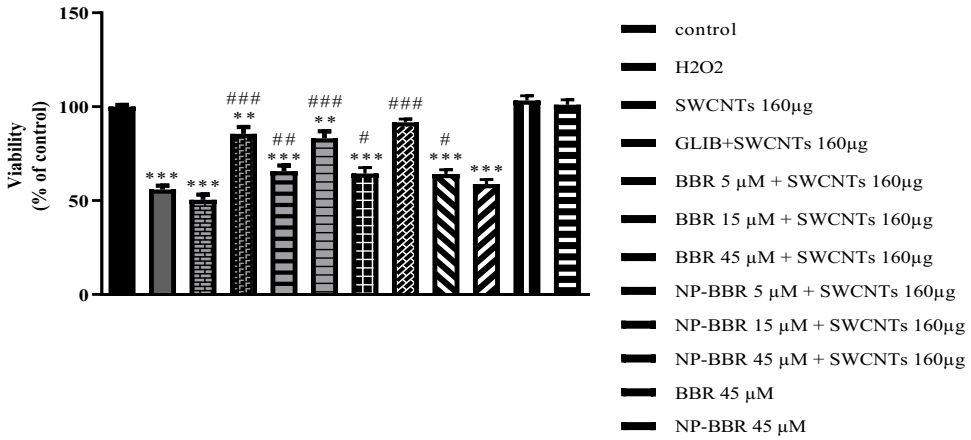

Fig. 8 Pretreatment effects of BBR (5, 15, and 45 μM), NP-BBR (5, 15, and 45 μM), and glibenclamide (GLIB, 10 μM) on cell viability of isolated pancreatic mice islets after 24-h exposure to SWCNT (160 μg). Results were expressed as mean ± SD (7 mice in each group). The difference between control and other groups was significant at $P < 0.01$ (**) and $P < 0.001$ (***). The difference between SWCNT and other groups was significant at $P < 0.05$ (#), $P < 0.01$ (##), and $P < 0.001$ (###). SWCNT, single-walled carbon nanotube; BBR, berberine; NP-BBR, berberine nanoparticle; GLIB, glibenclamide

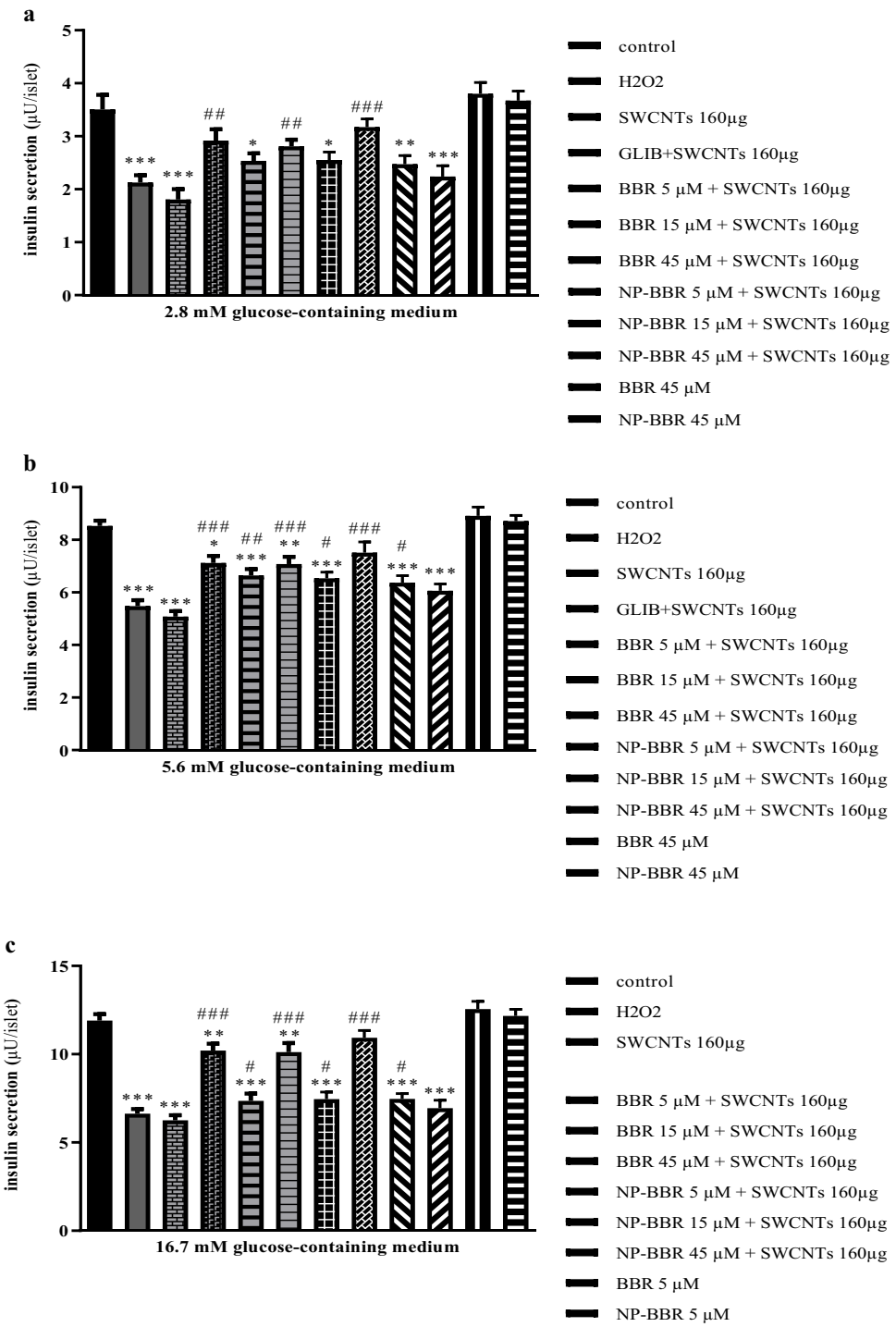

Fig. 9 Pretreatment effects of BBR (5, 15, and 45 μM), NP-BBR (5, 15, and 45 μM), and glibenclamide (GLIB, 10 μM) on insulin secretion of isolated pancreatic mice islets after 24-h exposure to SWCNT (160 μg) and a subsequent 1-h incubation with (**a**) 2.8 mM, (**b**) 5.6 mM, or (**c**) 16.7 mM glucose-containing medium. Results were expressed as mean ± SD (7 mice in each group). The difference between control and other groups was significant at $P < 0.05$ (*), $P < 0.01$ (**), and $P < 0.001$ (***). The difference between SWCNT and other groups was significant at $P < 0.05$ (#), $P < 0.01$ (##), and $P < 0.001$ (###). SWCNT, single-walled carbon nanotube; BBR, berberine; NP-BBR, berberine nanoparticle; GLIB, glibenclamide

effect was detected in the BBR 15 μM ($P < 0.01$) and NP-BBR 5 μM ($P < 0.01$) (Table 4). Pre-treatment with GLIB 10 μM, in all concentrations of glucose medium, significantly improved the SOD activity in comparison with the SWCNT group alone ($P < 0.05$, $P < 0.01$, and $P < 0.001$).

Effect of BBR and NP-BBR on GPx activity

GPx activity of islet significantly declined in the SWCNT group alone in comparison with the control group ($P < 0.001$). In concentrations of 2.8 and 5.6 μM glucose, GPx activity significantly improved after

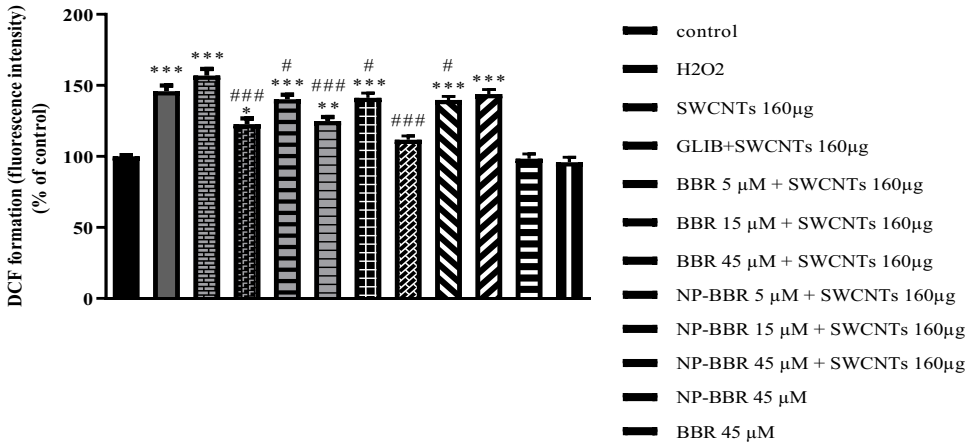

Fig. 10 Pretreatment effects of BBR (5, 15, and 45 µM) and NP-BBR (5, 15, and 45 µM), and glibenclamide (GLIB, 10 µM) on ROS levels in islets after 24-h exposure SWCNT (160 µg). Results were expressed as mean ± SD (7 mice in each group). The difference between control and other groups was significant at $P < 0.05$ (*), $P < 0.01$ (**), and $P < 0.001$ (***). The difference between SWCNT and other groups was significant at $P < 0.05$ (#) and $P < 0.001$ (###). SWCNT, single-walled carbon nanotube; BBR, berberine; NP-BBR, berberine nanoparticle; GLIB, glibenclamide

pre-treatment with BBR 15 µM, NP-BBR 5 µM, and GLIB 10 µM groups in comparison with the SWCNT group alone ($P < 0.05$, $P < 0.01$, and $P < 0.001$) (Table 2 and Table 3). But in concentration of 16.7 mM glucose, GPx activity significantly improved by BBR (5 and 15 µM), NP-BBR (5 µM), and GLIB (10 µM) groups in comparison with the SWCNT group alone ($P < 0.05$, $P < 0.01$, and $P < 0.001$) (Table 4).

Effect of BBR and NP-BBR on MDA levels

In all concentrations of glucose medium, the MDA levels pointedly augmented in the SWCNT group in comparison with the control group ($P < 0.001$). While in all concentrations of glucose medium, MDA levels of islets by pre-treatment with BBR (5, 15, and 45 µM), NP-BBR (5 and 15 µM), and GLIB (10 µM) significantly declined in comparison with

Table 2 Pretreatment islets with BBR (5, 15, and 45 µM), NP-BBR (5, 15, and 45 µM), and glibenclamide (GLIB, 10 µM) for 24 h and then treatment them with SWCNT (160 µg) for 24 h and a subsequent 1 h incubation with 2.8 µM glucose-containing medium

Groups	GSH (mg/mg protein)	MDA (nmol/mg protein)	CAT (U/mg protein)	SOD (U/mg protein)	GPx (U/mg protein)
Control	59.26 ± 3.35	6.22 ± 0.60	4.71 ± 0.53	40.20 ± 2.87	101.80 ± 4.41
SWCNT 160 µg	29.70 ± 4.70 *	10.60 ± 0.90 *	1.89 ± 0.22 *	19.42 ± 3.62 *	75.52 ± 5.30 *
SWCNT 160 + GLIB 10 µM	42.79 ± 6.68 ##	7.95 ± 0.82 ###	3.10 ± 0.45 ##	29.84 ± 5.42 ##	89.27 ± 4.41 ##
SWCNT 160 + BBR 5 µM	40.40 ± 5.12 #	8.85 ± 0.57 #	2.94 ± 0.37 #	27.71 ± 4. 92 #	85.83 ± 5.73
SWCNT 160 + BBR 15 µM	42.43 ± 6.65 ##	8.01 ± 1.14 ###	3.15 ± 0.55 d ##	31.26 ± 5.05 ###	87.97 ± 7.78 d #
SWCNT 160 + BBR 45 µM	39.89 ± 5.31 d #	8.80 ± 0.54 d #	2.81 ± 0.56	26.93 ± 2.57	84.23 ± 4.65
SWCNT 160 + NP-BBR 5 µM	51.30 ± 4.84 ###	6.94 ± 0.51 ###	3.97 ± 0.51 ###	35.24 ± 3.26 ###	93.19 ± 4.39 ###
SWCNT 160 + NP-BBR 15 µM	40.07 ± 4.06 d #	8.93 ± 0.70 d #	2.71 ± 0.53	27.58 + 4.51	82.73 ± 4.16
SWCNT 160 + NP-BBR 45 µM	34.92 ± 4.83	9.25 ± 0.70	2.45 ± 0.31	25.17 ± 3.23	79.10 ± 4.21
BBR 5 µM	63.79 ± 5.27	5.83 ± 0.82	5.02 ± 0.56	43.69 ± 4.53	104.70 ± 7.90
NP-BBR 5 µM	60.15 ± 4.37	6.07 ± 0.86	4.82 ± 0.48	41.36 ± 4.40	102.50 ± 7.31

Values expressed as mean ± SD

* $P < 0.001$ significant difference from the control group

# $P < 0.05$, ## $P < 0.01$, and ### $P < 0.001$ significant differences from the SWCNT group alone

Table 3 Pretreatment islets with BBR (5, 15, and 45 μM), NP-BBR (5, 15, and 45 μM), and glibenclamide (GLIB, 10 μM) for 24 h and then treatment them with SWCNT (160 μg) for 24 h and a subsequent 1 h incubation with 5.6 μM glucose-containing medium

Groups	GSH (mg/mg protein)	MDA (nmol/mg protein)	CAT (U/mg protein)	SOD (U/mg protein)	GPx (U/mg protein)
Control	61.07 ± 3.14	4.91 ± 0.68	4.93 ± 0.68	42.38 ± 3.50	104.8 ± 7.07
SWCNT 160 μg	32.28 ± 3.32 *	9.81 ± 0.64 *	2.21 ± 0.37 *	21.70 ± 2.52 *	78.65 ± 5.79 *
SWCNT 160 + GLIB 10 μM	45.23 ± 6.01 ##	6.64 ± 0.95 ###	3.82 ± 0.39 ###	32.92 ± 4.72 ###	93.57 ± 6.75 ##
SWCNT 160 + BBR 5 μM	43.65 ± 458 #	7.83 ± 0.97 ##	3.39 ± 0.40 ##	31.19 ± 3.67 #	89.50 ± 5.72
SWCNT 160 + BBR 15 μM	45.06 ± 9.69 ##	6.77 ± 0.98 ###	3.88 ± 0.61 ###	34.02 ± 4.04 ###	91.80 ± 6.34 #
SWCNT 160 + BBR 45 μM	43.44 ± 3.68 #	8.20 ± 0.74 #	3.31 ± 0.43 #	30.59 ± 4.02 #	87.61 ± 6.38
SWCNT 160 + NP-BBR 5 μM	54.52 ± 4.74 ###	5.91 ± 0.68 ###	4.28 ± 0.34 ###	37.67 ± 3.51 ###	95.87 ± 5.58 ###
SWCNT 160 + NP-BBR 15 μM	43.09 ± 3.66 #	8.07 ± 0.97 #	3.34 ± 0.38 #	30.30 ± 4.58 #	88.52 ± 4.90
SWCNT 160 + NP-BBR 45 μM	36.13 ± 4.17	8.46 ± 0.96	3.10 ± 0.55 #	27.85 ± 3.89	84.78 ± 4.39
BBR 5 μM	63.51 ± 4.25	4.62 ± 0.66	5.15 ± 0.63	44.78 ± 5.32	107.20 ± 7.00
NP-BBR 5 μM	61.93 ± 5.09	4.80 ± 0.39	5.02 ± 0.46	43.04 ± 5.15	105.70 ± 6.18

Values expressed as mean ± SD

* $P < 0.001$ significant difference from the control group

# $P < 0.05$, ## $P < 0.01$, and ### $P < 0.001$ significant differences from the SWCNT group

the SWCNT group alone ($P < 0.05$, $P < 0.01$, and $P < 0.001$) (Tables 2, 3, and 4).

Effect of BBR and NP-BBR on CAT activity

In all concentrations of glucose medium, after islet exposure with SWCNT, the CAT activity pointedly diminished in comparison with the control group ($P < 0.001$). In concentration of 2.8 mM glucose, a significant development in CAT activity was detected in BBR (5 and 15 μM), NP-BBR (5 μM), and GLIB (10 μM) in comparison with the SWCNT group alone ($P < 0.05$, $P < 0.01$, and $P < 0.001$) (Table 2). In concentration of 5.6 mM glucose, an important rise in CAT activity was detected in BBR (5, 15, and 45 μM), NP-BBR (5, 15, and 45 μM), and GLIB (10 μM) in comparison with the SWCNT group alone ($P < 0.05$, $P < 0.01$, and $P < 0.001$) (Table 3). While in concentration of 16.7 mM glucose, a remarkable increase in the CAT activity was only observed in BBR (15 μM), NP-BBR (5 μM), and GLIB (10 μM) in comparison with the SWCNT group alone ($P < 0.01$ and $P < 0.001$) (Table 4).

Discussion

The results of our study showed that SWCNT were able to induce oxidative stress, ROS formation, and decreased insulin secretion of β-cells. In the present study, pancreatic islet exposure with SWCNT (160 μg) significantly reduced insulin secretion after the addition of 2.8, 5.6, and 16.7 mM glucose. A similar study to our study showed that SWCNT caused oxidative stress in the pancreatic islets, decreased insulin secretion, and diabetes (Ahangarpour et al. 2018), while pre-treatment islets with BBR (5 and 15 μM) and NP-BBR 5 μM significantly decreased ROS generation, MDA levels and improved levels of GSH, SOD, GPx, and CAT, as well as increased insulin secretion.

There are several results of various scientific tests on cells and some results indicate that CNTs are highly toxic, but others have found no signs of toxicity Shvedova et al. 2003; Kagan et al. 2006. But our results on the viability of Langerhans islets β-cells with different concentrations of their SWCNT showed that cell viability of 40 μg of SWCNT was 94.6%, 80 μg of SWCNT was 84.8%, 160 μg of SWCNT was 48.8%, and cell viability of 320 μg of SWCNT was 40.3% compared to the control group with cell viability 100%. Consequently, 160 μg of SWCNT was considered the most effective and toxic dose. Our results show that SWCNT, which could induce oxidative stress and ROS production, were some of the main mechanisms that cause cell apoptosis; also, our results showed that these mechanisms caused damage to β-cells and reduced their insulin secretion. A similar study to our study showed that SWCNT with a concentration of 160 μg with oxidative stress mechanism caused toxicity in β-cells and decreased islet insulin secretion levels Ahangarpour et al. 2018.

Double emulsion-solvent evaporation using Eudragit RS 100 polymer was the technique used to make NP-BBR in

Table 4 Pretreatment islets with BBR (5, 15, and 45 μM), NP-BBR (5, 15, and 45 μM), and glibenclamide (GLIB, 10 μM) for 24 h and then treatment them with SWCNT (160 μg) for 24 h and a subsequent 1 h incubation with 16.7 μM glucose-containing medium

Groups	GSH (mg/mg protein)	MDA (nmol/mg protein)	CAT (U/mg protein)	SOD (U/mg protein)	GPx (U/mg protein)
Control	57.60 ± 6.84	7.31 ± 0.64	4.42 ± 0.58	38.20 ± 3.8	97.61 ± 7.03
SWCNT 160 μg	26.78 ± 4.80 *	12.55 ± 1.20 *	1.62 ± 0.40 *	18.39 ± 4.63 *	72.70 ± 7.58 *
SWCNT 160 + GLIB 10 μM	39.46 ± 5.69 ##	8. 25 ± 0.84 ###	2.71 ± 0.32 #	27.04 ± 4.28 #	87.29 ± 6.04 #
SWCNT 160 + BBR 5 μM	36.34 ± 3.70	10.11 ± 1. 07 #	2.53 ± 0.37	24.23 ± 3.77	83.08 ± 4.47 ###
SWCNT 160 + BBR 15 μM	40.39 ± 6.64 ##	8.99 ± 0.97 ###	2.87 ± 0.71 ##	27.90 ± 4.21 ##	86.11 ± 8.43 #
SWCNT 160 + BBR 45 μM	35.73 ± 4.96	10.14 ± 1.46 #	2.41 ± 0.39	23.73 ± 3.03	83.50 ± 1.94
SWCNT 160 + NP-BBR 5 μM	47.94 ± 5.37 ###	8.08 ± 0.89 ###	3.36 ± 0.27 ###	31.43 ± 4.24 ###	89.39 ± 6.35 ##
SWCNT 160 + NP-BBR 15 μM	35.68 ± 5.11	10.28 ± 1.18 #	2.45 ± 0.40	24.09 ± 3.49	83.07 ± 4.41
SWCNT 160 + NP-BBR 45 μM	31.79 ± 3.28	10.64 ± 1.53	2.26 ± 0.28	22.66 ± 3.79	80.01 ± 6.99
BBR 5 μM	59.96 ± 5.89	6.94 ± 0.64	4.74 ± 0.76	39.18 ± 5.23	100.20 ± 7.01
	58.49 ± 5.81	7.19 ± 0.64	4.58 ± 0.49	38.78 ± 4.63	98.56 ± 6.99

Values expressed as mean ± SD

* $P < 0.001$ significant difference from the control group

# $P < 0.05$, ## $P < 0.01$, and ### $P < 0.001$ significant differences from the SWCNT group

this study. The prepared nanoparticles were investigated and approved by the following studies: zeta potential evaluation, size evaluation, dispersity, morphology, drug release studies, and thermal gravimetric. Previous studies have shown that Eudragit RS-100 was used orally for the preparation of nanoparticles with double emulsion and solvent evaporation.

Toxicity of CNTs has been observed in a number of species. Studies have shown that oxidative stress, intracellular particle accumulation, and physical interaction of nanoparticles with cell surfaces and intracellular organelles were possible mechanisms of CNT toxicity Schwab et al. 2011. Considering previous studies, oxidative stress plays an important role in the damage caused by CNTs and can be used as a criterion for assessing their toxicity Nel et al. 2006. Some previous researches have shown that CNT-induced ROS production was actually related to the transfer metals released by these nanoparticles Liu et al. 2013. In addition, SWCNT as one of the nanoparticles have been shown to cause mitochondrial dysfunction, apoptosis, and cytotoxicity through the oxidative stress pathway. They have also shown that ROS production plays an important role in activating the mitochondrial-dependent apoptotic pathway Cheng et al. 2011. Studies have shown that contact of ROS with Langerhans β-cells could activate some pathways of cellular oxidative stress, which in turn has a significant effect on reducing islet insulin secretion Evans et al. 2002. High glucose levels have been reported to increase ROS production, either acutely or chronically in diabetes, thereby activating apoptotic pathways and cell death in β-cells Kohnert et al. 2012. In the present study, the islet exposure to SWCNT significantly decreased the insulin secretion after the addition of 2.8, 5.6, and 16.7 mM of glucose mediums. Due to the vulnerability of β-cells to oxidative stress and low amounts of antioxidants in this tissue, their contact to ROS can stimulate some cellular stress-sensitive pathways which are associated with decreased insulin secretion. It appears to be a relationship between K_{ATP} current and β-cell function in cases of mild oxidative stress. Low levels of ROS help β-cell function and the regulation of insulin gene expression. While high levels of ROS decrease insulin gene expression and insulin secretion, it leads to islet damage. The three factors of glucose metabolism, ROS production, and ATP production as a result of K_{ATP} channel activity are associated with β-cell dysfunction. SWCNT disrupt ATP production and open K_{ATP} channels, leading to hyperpolarization of β-cells to limit calcium influx and glucose-induced insulin secretion. Mitochondrial ROS accumulation followed by ATP depletion is associated with metabolism and cell death Ahangarpour et al. 2014, 2017. Our findings have shown that SWCNT as inducers of ROS decreased the insulin secretion of β-cell by generating the oxidative stress.

Antioxidant enzymes such as SOD, CAT, GPx, and non-enzymatic antioxidants such as GSH are the first line of antioxidant defense against the adverse effects of ROS in cells and play an important role in maintaining the stability of cellular homeostasis Guo et al. 2015.

Nanoparticle-related studies have shown that cell contact with SWCNT reduced the cells' primary antioxidant defenses including reduced CAT, GSH, SOD, and GPx levels Moller et al. 2014. The results of the present study showed that the activities of CAT, SOD and GPx, and GSH level in the islets were meaningfully diminished in contact with SWCNT (160 μg).

In recent years, several studies have shown the antioxidant and anti-inflammatory effects of BBR and its effectiveness on diabetes Shan et al. 2013. Previous studies have shown the effect of BBR on insulin resistance and dyslipidemia Lee et al. 2006. Studies have shown that BBR increased the expression of genes involved in insulin secretion, β-cell regeneration, increased insulin function in cells, and insulin-sensitive cells Zhou et al. 2009. BBR also improved metabolic syndrome, regulated glucose metabolism, lowered blood glucose levels, and prevented insulin resistance. One study showed that BBR was able to improve insulin resistance by regulating the expression of insulin receptor substrate 1 insulin and glucagon Gu et al. 2012. Although BBR has many beneficial properties, its clinical applications are limited due to its low bioavailability, low absorption, and low solubility in water. The aim of our study was to increase the properties of BBR and reduce its limitations by continuous release and improve its effectiveness on insulin secretion and oxidative stress by preparing its nanoparticles.

The hydrophilic nature of Eudragit RS-100 facilitates the solubility of BBR in the polymer matrix Perumal et al. 1999. Dehghani et al. showed that gallic acid-loaded Eudragit-RS 100 nanoparticles improved renal oxidative stress, inflammation, mitochondrial dysfunction, histopathological alterations, and biochemical tests induced by cisplatin better than gallic acid Dehghani et al. 2020. Findings of the current study showed that pretreatment with 5 and 15 μM of BBR and 5 μM of NP-BBR reduced ROS generation and MDA levels in islet, which indicated a reduction in oxidative stress by BBR and NP-BBR. In addition, the results of present study demonstrated that antioxidant enzyme activities including SOD and CAT were pointedly improved in BBR (5 and 15 μM) and NP-BBR (5 μM) groups in comparison with the SWCNT group alone that this indicated the antioxidative effects of BBR and NP-BBR on islet at low dose.

Conclusion

The findings of this study confirmed that SWCNT could directly target the function of pancreatic β-islets. SWCNT changed islet redox status by inducing ROS production and decreasing antioxidant defense also reduced islet insulin secretion, while BBR (5 and 15 μM) and NP-BBR (5 μg) significantly improved insulin secretion and ameliorated antioxidant defense of islets. However, our findings provided new insight regarding the antioxidant potential of BBR and NP-BBR as alternative in the prevention or treatment of diabetes. However, before its clinical application, it is necessary to study the exact mechanism of its effect on the improvement of β-cells and the molecular mechanisms involved in insulin secretion.

Acknowledgements This paper was extracted from the thesis by Mohammad Reza Niknejad.

Author contribution FG designed the study and wrote the protocol; HK performed the statistical analysis; MN and NS synthesized nano-berberine. AA., MD, and MN performed the experiment and wrote the first draft of the manuscript. All authors read and approved the final manuscript.

Funding The author disclosed receipt of the financial support for the research, from the Department of Pharmacognosy, Medicinal Plant Research Center, Faculty of Pharmacy (grant number: N-9708), Ahvaz Jundishapur University of Medical Sciences.

Ahvaz Jundishapur University of Medical Sciences,Ahvaz,Iran,N-9708,Fereshteh Golfakhrabadi

Declarations

Ethics approval Not applicable for this study.

Consent to participate Not applicable for this study.

Consent for publication Not applicable for this study.

Competing interests The authors declare no competing interests.

References

Abushouk AI, Salem AMA, Abdel-Daim MM (2017) Berberis vulgaris for cardiovascular disorders: a scoping literature review Iran J Basic. Med Sci 20:503. https://doi.org/10.22038/IJBMS.2017.8674

Ahangarpour A, Heidari H, Mard SA (2014) Progesterone and cilostazol protect mice pancreatic islets from oxidative stress induced by hydrogen peroxide. Iran J Pharm Res IJPR 13:937–945

Ahangarpour A, Oroojan AA, Rezae M, Khodayar MJ, Alboghobeish S, Zeinvand M (2017) Effects of butyric acid and arsenic on isolated pancreatic islets and liver mitochondria of male mouse. Gastroenterol Hepatol Bed Bench 10:1–44

Ahangarpour A, Alboghobeish S, Oroojan A, Dehghani M (2018) Mice pancreatic islets protection from oxidative stress induced by single walled carbon nanotubes through naringin. Human Exp Toxicol 37:1268–1281

Allegri M, Perivoliotis DK, Bianchi MG, Chiu M, Pagliaro A, Koklioti MA, Charitidis CA (2016) Toxicity determinants of multi-walled carbon nanotubes: the relationship between functionalization and agglomeration. Toxicol Reports 3:230–243. https://doi.org/10.1016/j.toxrep.2016.01.01

Anitha A, Deepagan V, Rani VD, Menon D, Nair S, Jayakumar R (2011) Preparation, characterization, in vitro drug release and biological studies of curcumin loaded dextran sulphate–chitosan nanoparticles. Carbohydr Polym 84:1158–1164. https://doi.org/10.1016/j.carbpol.2011.01.005

Armand J, Magnard F, Bouzon J, Rollet J, Taverdet J, Vergnaud J (1987) Modelling of drug release in gastric liquid from spheric galenic forms with Eudragit matrix. Int J Pharma 40:33–41

Babay D, Hoffman A, Benita S (1988) Design and release kinetic pattern evaluation of indomethacin microspheres intended for oral administration. Biomaterials 9:482–488. https://doi.org/10.1016/0142-9612(88)90042-7

Barzegar-Jalali M, Alaei-Beirami M, Javadzadeh Y, Mohammadi G, Hamidi A, Andalib S, Adibkia K (2012) Comparison of physicochemical characteristics and drug release of diclofenac sodium–eudragit® RS100 nanoparticles and solid dispersions. Powder Technol 219:211–216. https://doi.org/10.1016/j.powtec.2011.12.046

Baughman RH, Zakhidov AA, de Heer WA (2002) Carbon nanotubes–the route toward applications. Science 297:787–792. https://doi.org/10.1126/science.1060928

Beck LR, Cowsar DR, Lewis DH, Cosgrove RJ Jr, Riddle CT, Lowry SL, Epperly T (1979) A new long-acting injectable microcapsule system for the administration of progesterone. Fertil Steril 31:545–551. https://doi.org/10.1016/S0015-0282(16)44002-1

Bhaskar K, Anbu J, Ravichandiran V, Venkateswarlu V, Rao YM (2009) Lipid nanoparticles for transdermal delivery of flurbiprofen: formulation, in vitro, ex vivo and in vivo studies. Lipid in Health Dis 8:6

Bodmeier R, McGinity JW (1988) Polylactic acid microspheres containing quinidine base and quinidine sulphate prepared by the solvent evaporation method. III. Morphology of the microspheres during dissolution studies. J Microencapsul 5:325–330. https://doi.org/10.3109/02652048709021821

Bottini M, Bruckner S, Nika K, Bottini N, Bellucci S, Magrini A, Bergamaschi A, Mustelin T (2006) Multi-walled carbon nanotubes induce T lymphocyte apoptosis. Toxicol Lett 160:121–126. https://doi.org/10.1016/j.toxlet.2005.06.020

Bradford MM (1976) A rapid and sensitive method for the quantitation of microgram quantities of protein utilizing the principle of protein-dye binding. Anal Biochem 72:248–254

Carter JD, Dula SB, Corbin KL, Nunemaker CS (2009) A practical guide to rodent islet isolation and assessment. Biol Proced Online 11:3–11

Ceriello A & Testa R (2009)Antioxidant anti-inflammatory treatment in type 2 diabetes. Diabetes Care 32: dc09-S316. https://doi.org/10.2337/dc09-S316

Chen X, Zhang Y, Zhu Z, Liu H, Guo H, Xiong C, Su S (2016) Protective effect of berberine on doxorubicininduced acute hepatorenal toxicity in rats. Mol Med Rep 13:3953–3960

Cheng WW, Lin ZQ, Wei BF, Zeng Q, Han B, Wei CX, Xi ZG (2011) Single-walled carbon nanotube induction of rat aortic endothelial cell apoptosis: reactive oxygen species are involved in the mitochondrial pathway. Int J Biochem Cell Biol 43:564–572. https://doi.org/10.1016/j.biocel.2010.12.013

Danaei M, Dehghankhold M, Ataei S, Hasanzadeh Davarani F, Javanmard R, Dokhani A, Mozafari M (2018) Impact of particle size and polydispersity index on the clinical applications of lipidic nanocarrier systems. Pharmaceutics 10:57

DehghaniMaramMoghimipourKhorsandiMahdavinia MANSELM (2020) Protective effect of gallic acid and gallic acid loaded Eudragit RS 100 nanoparticles on cisplatin induced mitochondrial dysfunction and inflammation in rat kidney. Biochim et Biophysica Acta BBA Mol Basis Dis 1866:165911. https://doi.org/10.1016/j.bbadis.2020.165911

Evans JL, Goldfine LD, Maddux BA, Grodsky GM (2002) Oxidative stress and stress-activated signaling pathways: a unifying hypothesis of type 2 diabetes. Endocr Rev 23:599–622. https://doi.org/10.1210/er.2001-0039

Gu JJ, Gao FY, Zhao TY (2012) A preliminary investigation of the mechanisms underlying the effect of berberine in preventing high-fat diet-induced insulin resistance in rats. J Physiol Pharmacol 63:505–513

Guo C, Xia Y, Niu P, Jiang L, Duan J, Yu Y, Sun Z (2015) Silica nanoparticles induce oxidative stress, inflammation, and endothelial dysfunction in vitro via activation of the MAPK/Nrf2 pathway and nuclear factor-kappaB signaling. Int J Nanomedicine 10:1463–1477

Hosseini A, Baeeri M, Rahimifard M, Navaei-Nigjeh M, Mohammadirad A, Pourkhalili N, Abdollahi M (2013) Antiapoptotic effects of cerium oxide and yttrium oxide nanoparticles in isolated rat pancreatic islets. Hum Exp Toxicol 32:544–553. https://doi.org/10.1177/0960327112468175

Huang HP, Ghebre-Sellassie I (1989) Preparation of microspheres of water-soluble pharmaceuticals. J Microencapsul 6:219–225. https://doi.org/10.3109/02652048909098024

Jeyanthi R, Rao KP (1989) Release characteristics of bleomycin mitomycin C and 5-fluorouracil from gelatin microspheres. Int J Pharm 55:31–37

Johansen JS, Harris AK, Rychly DJ, Ergul A (2005) Oxidative stress and the use of antioxidants in diabetes: linking basic science to clinical practice. Cardiovasc Diabetol 4:1475–2840

JosPichardoPuerto SanchezGriloCamean ASMEAAM (2009) Cytotoxicity of carboxylic acid functionalized single wall carbon nanotubes on the human intestinal cell line Caco 2. Toxicol In Vitro 23:1491–1496. https://doi.org/10.1016/j.tiv.2009.07.001

Kagan VE, Tyurina YY, Tyurin VA, Konduru NV, Potapovich AL, Osipov AN, Kisin ER, Schwegler-Berry D, Mercer R, Castranova V (2006) Direct and indirect effects of single walled carbon nanotubes on RAW 264.7 macrophages: role of iron. Toxicol Lett 165:88–100. https://doi.org/10.1016/j.toxlet.2006.02.001

Kazuhiko J, Masahiro N, Miho K (1986) Controlled release of aclarubicim, an anticancer antibiotic, from poly-β-hydroxybutyric acid microspheres. J Control Release 4:25–32. https://doi.org/10.1016/0168-3659(86)90030-1

Kohnert KD, Freyse EJ, Salzsieder E (2012) Glycaemic variability and pancreatic beta-cell dysfunction. Curr Diabetes Rev 8:345–354

Kojima T, Nakano M, Juni K, Inoue S, Yoshida Y (1984) Preparation and evaluation in vitro of polycarbonate microspheres containing local anesthetics. Chem Pharm Bull 32:2795–2802. https://doi.org/10.1248/cpb.32.2795

Lee YS, Kim WS, Kim KH, Yoon MJ, Cho HJ, Shen Y, Kim JB (2006) Berberine, a natural plant product, activates AMP-activated protein kinase with beneficial metabolic effects in diabetic and insulin-resistant states. Diabetes 55:2256–2264

Liu Y, Zhao Y, Sun B, Chen C (2013) Understanding the toxicity of carbon nanotubes. Acc Chem Res 46:702–713. https://doi.org/10.1021/ar300028m

Mady O (2017) Ibuprofen encapsulation by Eudragit RS100 as microspheres: preparation and drug release. MOJ Bioequiv Availab 4:193–199

Mirhadi E, Rezaee M, Malaekeh-Nikouei B (2018) Nano strategies for berberine delivery, a natural alkaloid of Berberis. Biomed Pharmacother 104:465–473. https://doi.org/10.1016/j.biopha.2018.05.067

Moller P, Christophersen DV, Jensen DM, Kermanizadeh A, Roursgaard M, Jacobsen NR, Loft S (2014) Role of oxidative stress in carbon nanotube-generated health effects. Arch Toxicol 88:1939–1964

Nath B, Nath LK, Kumar P (2011) Preparation and in vitro dissolution profile of zidovudine loaded microspheres made of Eudragit RS 100, RL 100 and their combinations. Acta Pol Pharm 68:409–415

Nel A, Xia T, Madler L, Li N (2006) Toxic potential of materials at the nanolevel. Science 311:622–627. https://doi.org/10.1126/science.1114397

Nishioka Y, Kyotani S, Okamura M, Miyazaki M, Okazaki K, Ohnishi S, Ito K (1990) Release characteristics of cisplatin chitosan microspheres and effect of containing chitin. Chem Pharm Bull 38:2871–2873

Ogawa Y, Yamamoto M, Okada H, Yashiki T, Shimamoto T (1988) A new technique to efficiently entrap leuprolide acetate into microcapsules of polylactic acid or copoly (lactic/glycolic) acid. Chem Pharm Bull 36:1095–1103. https://doi.org/10.1248/cpb.36.1095

Ong LC, Chung FF, Tan YF, Leong CO (2016) Toxicity of single-walled carbon nanotubes. Arch Toxicol 90:103–118

Perumal D, Dangor C, Alcock R, Hurbans N, Moopanar K (1999) Effect of formulation variables on in vitro drug release and micromeritic properties of modified release ibuprofen microspheres. J Mcroencapsul 16:475–487. https://doi.org/10.1080/026520499288924

Poupot R, Bergozza D, Fruchon S (2018) Nanoparticle-Based Strategies to Treat Neuro-Inflammation Materials 11:270. https://doi.org/10.3390/ma11020270

Quesada I, Todorova MG, Alonso-Magdalena P (2006) Glucose induces opposite intracellular Ca2 concentration oscillatory patterns in identified a-and _-cells within intact human islets of Langerhans. Diabetes 55:2463–2469

Schwab F, Bucheli TD, Lukhele LP, Magrez A, Nowack B, Sigg L, Knauer K (2011) Are carbon nanotube effects on green algae caused by shading and agglomeration? Environ Sci Technol 45:6136–6144. https://doi.org/10.1021/es200506b

Seki T, Kawaguchi T, Endoh H, Ishikawa K, Juni K, Nakano M (1990) Controlled release of 3′, 5′-diester prodrugs of 5-fluoro-2′-deoxyuridine from poly-L-lactic acid microspheres.). J Pharm Sci 79:985–987

Shan CY, Yang JH, Kong Y, Wang XY, Zheng MY, Xu YG, Chen LM (2013) Alteration of the intestinal barrier and GLP2 secretion in Berberine-treated type 2 diabetic rats. J Endocrinol 218:255–262. https://doi.org/10.1530/JOE-13-0184

Shvedova A, Castranova V, Kisin E, Schwegler-Berry D, Murray A, Gandelsman V, Maynard A, Baron P (2003) Exposure to carbon nanotube material: assessment of nanotube cytotoxicity using human keratinocyte cells. J Toxicol Environ Health A 66:1909–1926. https://doi.org/10.1080/713853956

Singh J, Robinson DH (1988) Controlled release captopril microcapsules: effect of non-ionic surfactants on release from ethyl cellulose microcapsules. J Microencapsul 5:129–137. https://doi.org/10.3109/02652048809056476

Spenlehauer G, Veillard M, Benoit JP (1986) Formation and characterization of cisplatin loaded poly (d, l-lactide) microspheres for chemoembolization.). J Pharm Sci 75:750–755

Suzuki K, Price J (1985) Microencapsulation and dissolution properties of a neuroleptic in a biodegradable polymer, poly (d, l-lactide). J Pharm Sci 74:21–24. https://doi.org/10.1002/jps.2600740106

Tangvarasittichai S (2015) Oxidative stress, insulin resistance, dyslipidemia and type 2 diabetes mellitus. World J Diabetes 6:456–480. https://doi.org/10.4239/wjd.v6.i3.456

Thompson EA, Sayers BC, Glista-Baker EE, Shipkowski KA, Ihrie MD, Duke KS, Bonner JC (2015) Role of signal transducer and activator of transcription 1 in murine allergen-induced airway remodeling and exacerbation by carbon nanotubes. Am J Respir Cell Mol Biol 53:625–636

Uchida T, Goto YT, S, (1992) Utility of mixture of commercially available polymers as constituents of sustained-release microcapsules containing cefadroxil or theophylline. Chem Pharm Bull 40:463–466. https://doi.org/10.1248/cpb.40.463

Vessby J, Basu S, Mohsen R, Berne C, Vessby B (2002) Oxidative stress and antioxidant status in type 1 diabetes mellitus. J Intern Med 251:69–76

Wada R, Hyon SH, Ikada Y (1990) Lactic acid oligomer microspheres containing hydrophilic drugs. J Pharm Sci 79:919–924. https://doi.org/10.1002/jps.2600791016

Whitesides GM (2003) The 'right' size in nanobiotechnology. Nat Biotechnol 21:1161–1165

Wolf G, Aumann N, Michalska M, Bast A, Sonnemann J, Beck JF, Walther R (2010) Peroxiredoxin III protects pancreatic ss cells from apoptosis. J Endocrinol 207:163–175. https://doi.org/10.1677/joe-09-0455

XiongGanYangXu FLLXLHB (2006) Puerarin protects rat pancreatic islets from damage by hydrogen peroxide. Eur J Pharmacol 529:1–7. https://doi.org/10.1016/j.ejphar.2005.10.024

Zhang W, Li X, Ye T, Chen F, Yu S, Chen J, Liu J (2014) Nanostructured lipid carrier surface modified with Eudragit RS 100 and its potential ophthalmic functions. Int J Nanomed 9:4305. https://doi.org/10.2147/IJN.S63414

Zhou J, Zhou S, Tang J, Zhang K, Guang L, Huang Y, Li D (2009) Protective effect of berberine on beta cells in streptozotocin- and high-carbohydrate/high-fat diet-induced diabetic rats. Eur J Pharmacol 606:262–268. https://doi.org/10.1016/j.ejphar.2008.12.056